2019 IEEE 69th Electronic Components and Technology Conference (ECTC)

Nanoscale Topography Characterization for Direct Bond Interconnect

Bongsub Lee, Pawel Mrozek, Gill Fountain, John Posthill,
Jeremy Theil, Guilian Gao, Rajesh Katkar, and Laura Mirkarimi
Xperi Corporation
San Jose, California, USA
bongsub.lee@xperi.com

***Abstract*—Hybrid bonding achieves mechanical and electrical connection between device wafers or dies, by directly joining dielectric and metal surfaces to form an all-inorganic interface. This direct bond interconnect (DBI) technology enables very fine pitch interconnects for high bandwidth interfaces. DBI is currently used for mass production of image sensors and is actively investigated for NAND, DRAM and MEMS applications. Characterizing and controlling nanoscale topography are essential for this type of bonding. After chemical mechanical polishing (CMP), the dielectric surface (usually SiO_2) should have high planarity and sub-nm roughness, and the metal surface (usually Cu) should be slightly recessed below the dielectric surface in general. Atomic force microscopy (AFM) is a critical technique required to monitor the CMP process module and ensure a robust manufacturing process. While AFM and related techniques have been known for decades, nanoscale or sub-nm scale characterization for DBI requires careful choice of the analysis configurations and parameters to avoid misinterpretation. Here we discuss key considerations for AFM analysis, extraordinary AFM artifacts in the relative heights of the Cu and SiO_2 areas, and topographic characteristics of Cu/SiO_2 surface for successful hybrid bonding. The force between an AFM tip and a sample should be sufficiently low for consistent roughness measurement but sufficiently high for minimizing the effects of surface contamination or artifacts. Proper data processing such as flattening should be done to make realistic images. Occasionally we observed artifacts that produced an incorrect Cu height, which could render an actually recessed Cu area as protruding. This artifact tends to occur more if the tip is not fresh or the tapping force is low. If a data image is unusually blurry and the oxide roughness is much smaller than usual, it may be a sign of this artifact. Replacing the tip or scanning in contact mode can usually demonstrate if there was an artifact. AFM analysis revealed that a curved SiO_2 surface tends to occur in the vicinity of Cu interconnect areas. Optimized CMP conditions can reduce the size of seams and eliminate them.**

Keywords—Hybrid bonding; nanoscale topography; 3D-IC; atomic force microscopy

I. INTRODUCTION

Hybrid bonding, or Direct Bond Interconnect (DBI), is currently used for mass production of CMOS image sensors for mobile phones [1] and is actively investigated for other 3-dimensional integrated circuit (3D-IC) applications such as 3D NAND [2] and die-to-wafer stacked DRAM [3][4]. Wafer or chip surfaces are polished, chemically activated, and then bonded at room temperature with almost no force. This room-temperature bonding already provides sufficient strength for normal handling. After many chips are bonded, they can be batch-annealed to achieve full mechanical strength and electrical connection [5] [6] [7]. This bonding technique forms a completely inorganic interface, without involving solder bumps or organic underfill between layers. Compared to the current solder-based stacking technology, hybrid bonding provides much finer pitch, higher bandwidth, better thermal performance, improved RLC characteristics, and higher assembly throughput [3].

Characterizing and controlling nanoscale topography is critical for the direct bond interconnect technology. In the case of simple dielectric-to-dielectric bonding (called direct bonding or ZiBond), the dielectric surface should be extremely smooth before activation and bonding. To achieve electrical connection between stacked layers (called hybrid bonding or DBI), the surface should have dielectric background areas (usually SiO_2) as well as metal pad areas (usually Cu). Chemical mechanical polishing (CMP) should achieve a very low dielectric roughness and also a certain recess of metal areas below the dielectric surface [8], which is illustrated in Fig. 1(a). Upon contact, the plasma-activated dielectric surfaces bond together instantaneously (Fig. 1(b)). Metal-to-metal bond occurs during a subsequent batch annealing. The coefficient of thermal expansion of metals are typically far larger than dielectrics. The metal expands to fill the gap and then build up internal pressure (Fig. 1(c)). It is under this internal pressure and annealing temperature that metal atoms diffuse across the interface, making good metal-to-metal bond and hence electrical connection. External pressure is not required for this type of bonding.

Atomic force microscopy (AFM) is a surface characterization tool that can monitor the nanoscale topography resulting from CMP. AFM analyzes topography by tracking the interaction between an ultra-sharp tip and surface atoms. While AFM and related techniques have been known for decades, we find that AFM characterization for DBI requires careful consideration of the analysis procedure and parameters to avoid misinterpretation. In this study, we discuss key considerations for AFM analysis and demonstrate surface topography characteristics of Cu/SiO_2 DBI surfaces. During CMP, relative removal rate of metal, dielectric, and barrier materials should be controlled to achieve the required topography for DBI. CMP may

2377-5726/19/$31.00 ©2019 IEEE
DOI 10.1109/ECTC.2019.00163

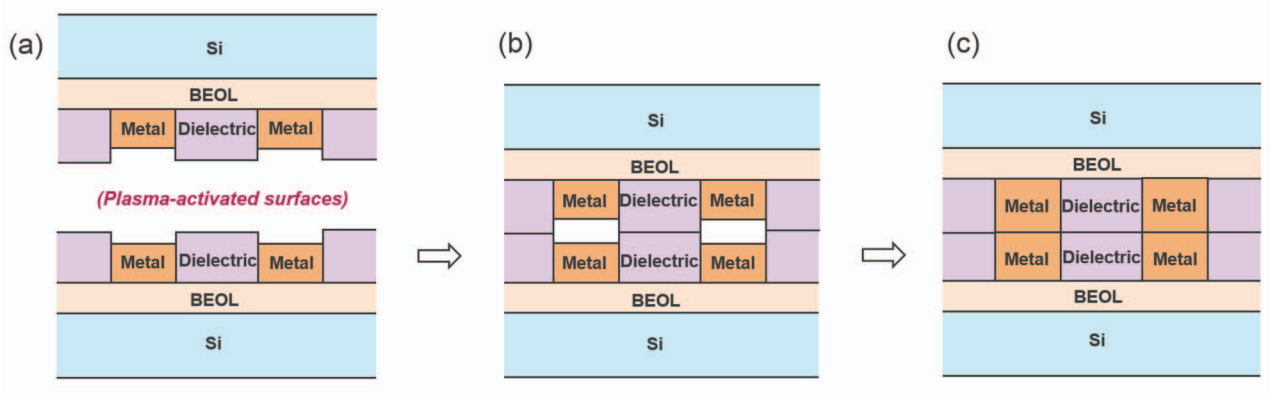

Figure 1. Schematic flow for Direct Bond Interconnect (DBI) process. (a) CMP prepares flat dielectric surfaces as well as moderately recessed metal surfaces. The surfaces are cleaned and plasma-activated (or activated by wet chemistry). (b) The surfaces are brought into contact. Dielectric surfaces bond together instantaneously at room temperature. (c) Upon batch annealing, the metal expands more than the dielectric and becomes internally pressurized. Metal-to-metal bonding is accomplished under this temperature and internal pressure (without external pressure). The initial metal recess has to be carefully controlled to make this process possible at a moderate annealing temperature.

produce a curved profile of oxide. We illustrate the effect of such curved profiles on the final bond interface. We also report occurrence of extraordinary AFM artifact from DBI structures. It can falsely indicate significant protrusion of Cu over SiO_2 and excessively smooth SiO_2 surface. We present examples of this artifact and discusses how to identify such problems.

II. Experiments: Considerations for AFM to Characterize Nanoscale Topography for DBI

A. Scanning Process for AFM

Fig. 2(a) is one example of 3-dimensional representation of a DBI sample surface, which can be constructed by AFM. It consists of a dielectric area (SiO_2) and evenly distributed metal pads (Cu). The metal pads are slightly recessed from the dielectric background, as depicted in Fig. 1(a). Fig. 2(b) is a magnified view of a small dielectric area. The root-mean-square roughness of the dielectric surface can be obtained by calculating the standard deviation of the z-values from each pixel. Note that it is popular to use μm as the x/y-axis unit and use nm or Å as the z-axis unit to show AFM results. The appearance of surface features is hence highly magnified along the z-axis in this kind of visual representation.

To properly understand the topography of a DBI structure by AFM, it is important to understand how to obtain height information and how to post-process the acquired data. The AFM tip scans the sample in one direction (usually in the x-direction) and obtain the height (z) information along that direction, as depicted in Fig. 3(a). Then the tip or the sample shifts in the orthogonal direction (usually in the y-direction) and repeats the x-scan there. Fig. 3(b) shows schematic examples of such x-z profiles. By stacking many x-z profiles together in the y-direction, one can obtain a 3-dimensional representation such as Fig. 3(c), which is an equivalent of Fig. 2(a). In Fig. 3(c), darker contrast represents lower points, and brighter contrast shows higher points.

B. Flattening Operation and Height Measurement

Combining AFM line profiles, as illustrated in Figs. 3(b) and 3(c), is usually accomplished by a "flattening" operation included in AFM analysis software [9]. If the AFM instrument can keep the relative height information from all points of the x-y plane, we will be able to see the entire 3-dimensional surface without distortion. One should adjust the sample tilt, since the sample plane cannot be perfectly perpendicular to the z-axis for measurement. This process is usually done by selecting the "whole" or "whole plane" option for flattening. However, while the relative height information is quite well preserved in the scanning direction (x-direction in this example), it is not always the case in the other direction (y-direction). For example, after

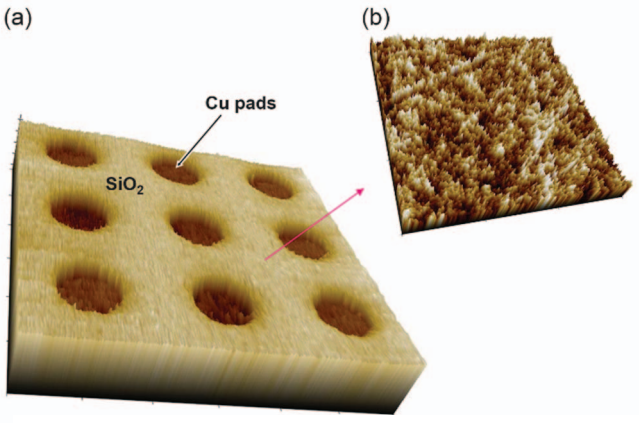

Figure 2. Examples of 3-dimensionally represented AFM data from a DBI sample. (a) Topography of an area of a DBI sample, which consists of SiO_2 background and recessed Cu pads. The size and pitch of Cu pads can vary widely depending on applications. (b) Magnified view of a small SiO_2 area. It is common to use μm as the x/y-axis unit and use nm or Å as the z-axis unit.

a tip spends time to obtain many profiles, the sample temperature may change slightly. Even infinitesimally small temperature fluctuation (or other kinds of fluctuation) may effectively shift the measured height in the nanometer scale. Such difference may happen between the times to obtain the first profile and the last profile of Fig. 3(b); the height relationship between the profiles (i) and (vi) is not always clear.

A popular method of combining profiles is "line-by-line" flattening. In general, it takes each x-z profile and corrects its tilt (line-by-line) and, when combining those x-z profiles, it relies on the user's definition of the relationship between the profiles. Most AFM operators are accustomed to performing line-by-line flattening after selecting the entire area. It fits all x-z profiles into a single plane by least squares fitting. In other words, the software obtains the average height in each profile and aligns all of the profiles at their averages. It is indeed a good way to obtain results like Fig. 2(b); it is reasonable to assume that all x-z profiles have the same average height. On the other hand, this simple method was not adequate for the DBI profiles in Fig. 3(b). The average of heights in the profile (iii) should be clearly different from that of (v). If one aligns all profiles at their average values (i.e. tries to fit all profiles into one plane by least squares fitting), the result will look like Fig. 3(d), which is clearly unrealistic with "leveling artifacts [9]". Instead, we typically aligned the profiles by selecting only a part of SiO_2 areas as shown in Fig. 3(e) and performing line-by-line flattening. It fits only the selected areas into one plane by least squares fitting, to construct a result like Fig. 3(c). This is a robust way to make a visually reasonable AFM image. This is still not completely accurate in the y-direction but does not include the effects of uncontrollable fluctuation of conditions. Whichever flattening method is used, the height relationship between different profiles (y-z information) is not very dependable.

To obtain Cu recess below the SiO_2 surface, one should measure the height difference between points along the scanning direction (e.g. within one x-z profile such as the profile (iii) in Fig. 3(b)), instead of trying to compare points at different y-locations. If one must compare points at different y values, the operator should align those points along the scan direction by rotating the sample before scanning. Some machines also allow users to scan along an arbitrary direction. In this work, we consistently scanned along one direction that Cu pads are aligned to.

We employed an AFM with a flexure scanner for this study and always used first-order data flattening. It only corrects the tilting (slope) of the sample. Many traditional AFM systems have a tube scanner, which makes a pendulum-like motion while scanning. With that, a scanned profile along a perfectly flat surface would look like a parabola instead of a straight line. While second-order flattening method has been commonly employed to correct this effect, this method is complicated when the sample surface has some curvature. Flexure scanners do not have this curved background issue, while they may still show a slightly uneven background from a flat sample due to mechanical imperfection (out-of-plane motion), e.g. about a couple of nm in z out of 100 μm in x. A proper flattening protocol should be chosen depending on the machine type. Good practice includes scanning a flat sample, such as a blank silicon wafer or an optical flat, to check the inherent background profile from the machine on a routine basis.

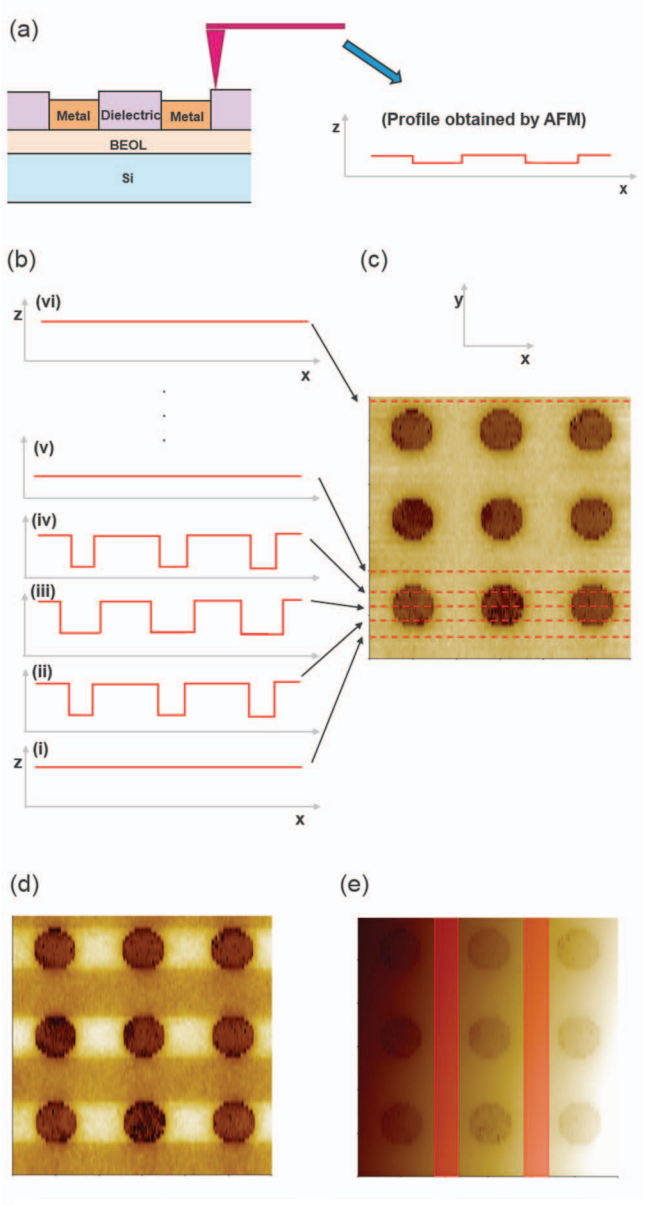

Figure 3. Method to construct a 3-dimensional representation of a DBI sample surface from AFM scans. (a) Obtaining a surface profile by scanning a sample surface. After taking one x-z profile, scanning can be repeated at different y-positions. (b) Schematic examples of surface profiles (x-z profiles). In actual AFM scanning, (c) Collection of many x-z profiles that shows the x, y, z information together. This is an equivalent 2D representaion of Fig. 2(a). (d) Result of a common line-by-line flattening, which selected the entire area and fitted them into a flat plane by least squares fitting. It gave visual artifacts (horizontal lines) for a typical DBI case. (e) Line-by-line flattening that was used to produce the result in c. Only the shaded SiO_2 areas were selected and fitted to a flat plane.

C. *Imaging Mode for DBI Samples*

We employed tapping, non-contact, and contact modes of AFM for this study. Tapping mode is the most popular imaging mode for AFM. The cantilever oscillates near its resonance frequency, and the tip "taps" on the surface [9]. Non-contact mode (or "true non-contact mode") operates at a larger distance where attractive force is dominant instead of repulsive force. Since the tip does not effectively touch the surface, this mode allows a very long tip life without mechanical wear. Note that an AFM tip has nanometers of radius, which can increase by mechanical wear. When a tip becomes less sharp, it cannot track very fine surface features, often measuring a lower roughness from the same surface. Non-contact mode was sometimes useful to measure dielectric roughness of many DBI samples consistently. However, this mode was often too sensitive to the surface conditions including slight contamination by organic substances and was prone to the interaction-force-related artifacts discussed in Section IV. The sensitivity of non-contact mode may be advantageous for very soft samples, but it is unnecessary for DBI sample surfaces that consist of relatively hard materials (SiO_2 and Cu). On the other hand, contact mode does not use oscillation. The tip "drags" on the surface with a relatively large force. The tip wears out quickly in contact mode, so it was not suitable for measuring roughness from multiple areas. It was robust for measuring Cu recess and especially useful to minimize the effects of organic contamination or force-related artifacts. When the data from contact and tapping modes were obviously different, the issue was due to degraded tip or surface condition.

For the purpose of DBI surface characterization, tapping mode AFM was a good compromise to obtain recess, roughness, and other surface characteristics from multiple areas with relatively good consistency. We replaced the tip after a certain amount of use before the measured roughness became too low, i.e. before the tip was worn out. When an artifact was suspected, we replaced the tip or tested the sample in contact mode.

III. Extraordinary Artifacts in AFM Data in DBI Structures

The validity of AFM data is critical in developing the CMP process for DBI. It is therefore important to understand all possible AFM artifacts. For example, it is well known that a worn-out tip may measure a low roughness value from an unacceptably rough sample.

In this study, we occasionally observed AFM artifacts that produced incorrect Cu recess values. It could even reverse the contrast, making recessed Cu areas appear as protruded. This type of artifact is not widely known with most AFM users and may cause significant misinterpretation. Fig. 4(a) is an example of normal AFM result from a DBI sample, showing recessed Cu areas. In some cases, the same sample showed completely different results as shown in Fig. 4(b). The Cu areas appear to be much higher than in the normal result, showing artificial protrusion in this case. The oxide roughness also appeared

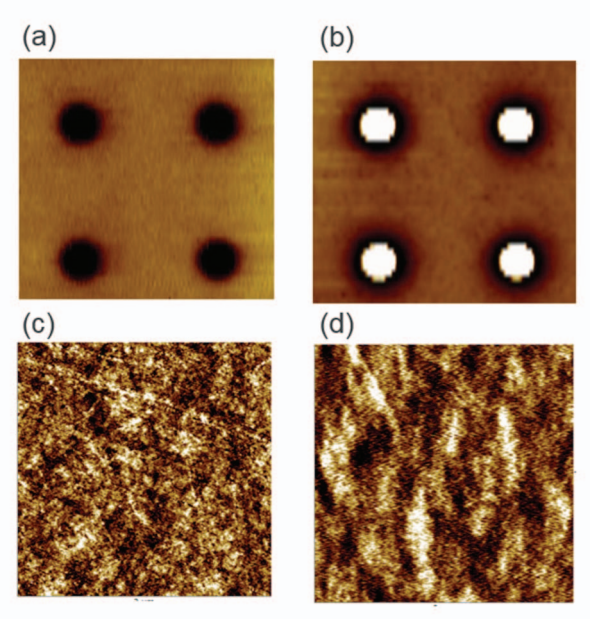

Figure 4. AFM artifacts due to abnormal tip-to-sample interaction. (a) Normal AFM result from a DBI sample with recessed Cu areas. (b) Erroneous AFM result from the sample sample, showing protruding Cu areas. (c) Normal AFM result from a small SiO_2 area of the same sample. (d) AFM result from a small SiO_2 area taken after the artifact was observed. The image is blurry, and the resulting roughness is lower than normal.

lower when this artifact occurred. Fig. 4(c) is a regular AFM result from a small SiO_2 area on this sample, and Fig. 4(d) is an erroneous result. Fig. 4(d) appears blurry and shows a lower roughness, while Fig. 4(c) is crisp and reveals actual surface features such as nanoscale scratches from CMP.

We have also observed a reversible behavior with such artifact. Fig. 5 shows two AFM results from the same area. In the case of Fig. 5(a), the scan started from the bottom and showed artificial protrusion. After the tip hit a large particle (or particles, shown with an arrow), the artifact suddenly disappeared and Cu recess was shown. After that, the same area was scanned again from the bottom for Fig. 5(b). Normal Cu recess was shown at first but, after the tip hit the particle again, artificial protrusion reappeared. This repetition occurred also from additional scans on this area.

Occurrence of this artifact was related to tip freshness and tip-sample interaction force. This artifact did not occur with an unused tip. It occurred with some tips after used for a certain amount, but it was difficult to predict how soon it could occur. Non-contact mode appeared more prone to this artifact. In one case, the artifact occurred only after scanning a couple of areas in a non-contact mode. When we switched to tapping mode with the same tip, the artifact disappeared. The artifact could occur also in tapping mode after some use. Contact mode was the most robust against this type of artifact.

The origin of this artifact is not fully known to us, but it should be related to the difference between the tip-Cu interaction and the tip-SiO_2 interaction in certain circumstances. One explanation is electrical charging near

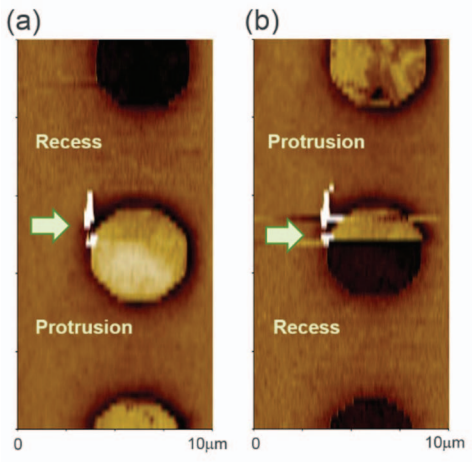

Figure 5. A case of reversible artifact. (a) AFM result that first showed artificial protrusion (bottom) then normal Cu recess (top) after the tip hit a large particle. (b) AFM result taken immediately afterward. The scan first showed normal recess at the bottom then artificial protrusion after the tip hit the same particle.

the AFM tip. A charged tip will interact differently on metal and dielectric areas on a DBI sample and have more difficulty in correctly analyzing roughness or nanoscale scratches (Fig. 4(c) and (d)). Charging may occur more easily with a used tip as it collects contaminants or become damaged after multiple scans. Non-contact mode should be more affected to the electrostatic force than contact mode. We tried using an ionizing air blower to remove static charges and observed limited improvement. It reduced the amount of artificial protrusion but did not completely remove the problem even after many minutes of exposure. As discussed in the previous section, tapping mode is the preferred method for general analysis of DBI structures, even though this artifact may occur. A good practice is to observe dielectric roughness over the course of measurements. If the data image is unusually blurry and the oxide roughness is much smaller than normal, it may be a sign of the artifact. Replacing the tip or testing with contact mode can usually demonstrate whether the feature is real or an artifact.

IV. Nanoscale Characteristics of Cu/SiO_2 DBI Surfaces and Their Effects on Bonding

For DBI, large deviations from flatness can affect the bond quality and bond strength. Curvature of the dielectric surface can affect the bond result but has not been discussed in detail in previous studies. Height change from SiO_2 to Cu may not usually be a strict step function especially when interacting with the CMP slurry. Therefore, the dielectric surface may become curved in the vicinity of metal interconnect areas. After initial bonding and annealing, this non-flatness may result in confined non-bonded areas or seams.

We developed multiple DBI designs and the corresponding CMP processes [3]. The dependence of layout and design on the resulting topography is well known in the CMP industry [10]. AFM measurements must be performed in conjunction with the CMP development. Die bonded with non-optimized CMP leave seams as shown in Fig. 6(a). The seam is described as a non-bonded SiO_2-to-SiO_2 area. In Fig. 6, the seams are observed near Cu areas. In the case of Fig. 6(b), the CMP condition was tuned to make much flatter oxide. It was also possible to minimize the occurrence of seams, depending on CMP conditions and DBI design. The example shown in Fig. 6(c) has no visible seams at the bond interface. Optimizing the CMP condition is the key to produce the right amount of surface characteristics such as metal recess, dielectric roughness, and dielectric curvature for DBI.

V. Conclusions

AFM is a critical technique to characterize the nanoscale topography for hybrid bonding. Careful protocols should be followed to ensure that the AFM characterization is accurate without artifacts that result in misleading interpretation. The force between an AFM tip and a sample should be sufficiently low for consistent roughness measurement but sufficiently strong for minimizing the effects of surface contamination or artifacts. Tapping mode was usually a good compromise for the purpose of DBI characterization. It is possible to produce a 3-dimensional representation of a surface by stacking many profiles. One should note that, in such a 3D representation, the height relationship is far more accurate within one profile than between different profiles. Accordingly, comparison of

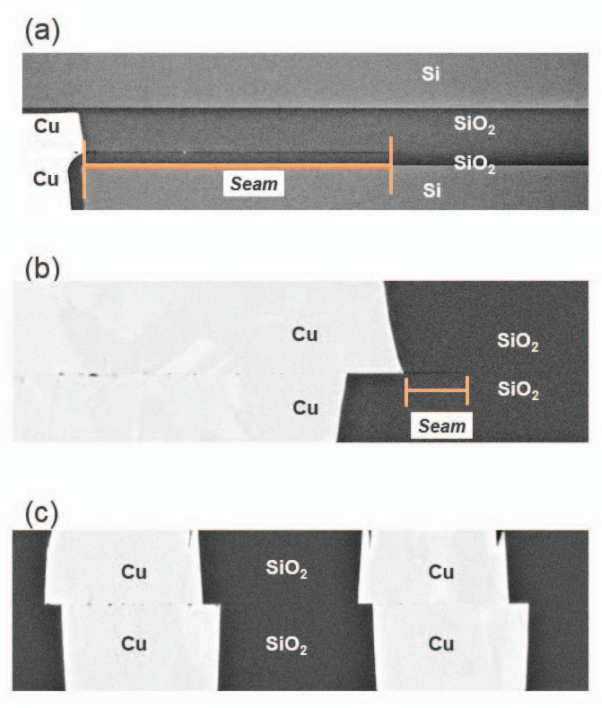

Figure 6. Cross-sectional scanning electron microscope images of DBI pairs. (a) Significant non-bonded SiO_2 area (seam) near the Cu pads. (b) Minimal seam during bond. (c) DBI pair without visible seams due to optimized CMP conditions.

heights should be done by comparing points along the scanning direction.

Occasionally we observed AFM artifacts that produced an incorrect Cu height, often showing artificial Cu protrusion from a truly recessed region. The artifact tends to occur more if the tip is not fresh or the tapping force is low. It is possibly due to local charging of the tip. Using an ionizer could reduce the degree of this artifact but did not completely remove it in our case. This artifact usually accompanies blurriness and excessively low roughness, so it is a good practice to watch the roughness in the course of scanning many areas. Replacing the tip or testing in contact mode can usually demonstrate whether there was an artifact.

Topographic metrology and AFM analysis are critical to characterize the CMP process which ultimately impacts that quality of the bond. By optimizing CMP conditions with the topographic metrics of roughness, flatness, and recess, we could eliminate the bond seams.

ACKNOWLEDGMENT

We thank Michael Huynh and Benny Fuentes for their help in sample preparation and SEM imaging, and Kang-Deuk Choi, Ardavan Zandiatashbar, Phani Kondapani, and David Braunstein for discussions.

REFERENCES

[1] P. Garrou, "IFTLE 303 Sony Introduces Ziptronix DBI Technology in Samsung Galaxy S7," Solid State Technology, 2016. http://electroiq.com/insights-from-leading-edge/2016/09/iftle-303-sony-introduces-ziptronix-dbi-technology-in-samsung-galaxy-s7/.

[2] R. Merritt, "YMTC Adds Detail to NAND Plans, EE Times," 2018. https://www.eetimes.com/document.asp?doc_id=1333563.

[3] G. Gao, L. Mirkarimi, G. Fountain, L. Wang, C. Uzoh, T. Workman, G. Guevara, C. Mandalapu, B. Lee and R. Katkar, "Scaling Package Interconnects Below 20μm Pitch with Hybrid Bonding," in IEEE 68th Electronic Components and Technology Conference, San Diego, 2018.

[4] B. Lee, R. Katkar, G. Gao, G. Fountain, S. Lee, L. Wang, C. Mandalapu, C. Uzoh, L. Mirkarimi, B. Sykes, M. Litjens, Y. Niu, S. Shao, J. Wang and S. Park, "Mechanical Strength Characterization of Direct Bond Interfaces for 3D-IC and," in Proc. IEEE 68th Electronic Components and Technology Conference, San Diego, 2018.

[5] V. Masteika, J. Kowal, N. S. J. Braithwaite and T. Rogers, "A Review of Hydrophilic SiliconWafer Bonding," ECS J. Solid State Sci. and Technol., vol. 3, no. 4, pp. Q42-Q54, 2014.

[6] P. Enquist, "Scalability and Low Cost of Ownership Advantages of Direct Bond Interconnect (DBI®) as Drivers for Volume Commercialization of 3-D Integration Architectures and Applications," in Materials Research Society Fall Meeting, 2008.

[7] P. Enquist, G. Fountain, C. Petteway, A. Hollingsworth and H. Grady, "Low Cost of Ownership Scalable Copper Direct Bond Interconnect 3D IC Technology for Three Dimensional Integrated Circuit Applications," in IEEE International Conference on 3D System Integration, 2009.

[8] P. Enquist, "3D Technology Platform – Advanced Direct Bond Technology," in 3D Integration for VLSI Systems, Pan Stanford Publishing, 2011, p. 175.

[9] P. Eaton and P. West, Atomic Force Microscopy, Oxford University Press, 2010.

[10] T.-C. Chen, M. Cho, D. Z. Pan and Y.-W. Chang, "Metal-Density-Driven Placement for CMP Variation and Routability," IEEE Trans. on Computer-Aided Design of Integ. Circ. and Sys., vol. 27, no. 12, pp. 2145-2155, 2008.